International Journal of Pharmaceutics 420 (2011) 161–171

Contents lists available at SciVerse ScienceDirect

International Journal of Pharmaceutics

journal homepage: www.elsevier.com/locate/ijpharm

Pharmaceutical nanotechnology

Self-nanoemulsifying drug delivery system of persimmon leaf extract: Optimization and bioavailability studies

Wanwen Li, Shaoling Yi, Zhouhua Wang, Si Chen, Shuang Xin, Jingwen Xie, Chunshun Zhao*

School of Pharmaceutical Sciences, Sun Yat-sen University, 132 Waihuan East Road, Guangzhou Higher Education Mega Center, GuangZhou 510006, PR China

ARTICLE INFO

Article history:
Received 1 March 2011
Received in revised form 27 July 2011
Accepted 16 August 2011
Available online 22 August 2011

Keywords:
Persimmon leaf extract
Self-nanoemulsifying drug delivery system
Extreme vertices mixture design
Bioavailability
Quercetin
Kaempferol

ABSTRACT

In current study, a self-nanoemulsifying drug delivery system (SNEDDS) of persimmon (*Diospyros kaki*) leaf extract (PLE) was developed and characterized to compare its *in vitro* dissolution and relative bioavailability with commercially available tablets (Naoxinqing tablets). Pseudo-ternary phase diagrams were constructed by phase diagram by micro plate dilution (PDMPD) method, of which the evaluation method was improved to use Multiskan Ascent for identifying turbidity. The formulation of PLE-loaded SNEDDS was optimized by an extreme vertices experimental design. The optimized nanoemulsion formulation, loading with 44.48 mg/g PLE total flavonoids, consisted of Cremophor EL, Transcutol P, Labrafil M 1944 CS (56:34:10, w/w), and it remained stable after storing at 40 °C, 25 °C, 4 °C for at least 6 months. When diluted with water, the SNEDDS droplet size was 34.85 nm and the zeta potential was −6.18 mV. Compared with the commercial tablets, the AUC of both quercetin and kaempferol, which are representative active flavonoids of PLE, was increased by 1.5-fold and 1.6-fold respectively following oral administration of PLE-loaded SNEDDS in fasting beagle dogs. These results indicate that SNEDDS is a promising drug delivery system for increasing the oral bioavailability of PLE.

1. Introduction

The PLE, extracted from the leaves of *Diospyros kaki* L. *Dispryosl* and *Ebenaceae*, is a mixture consisting mainly of flavonoids oligomers, organic acids, tannins, phenols, chlorophyll, vitamin C and caffeine (Lee et al., 2006). The PLE total flavonoids, including quercetin and its glycosides (hyperin, isoquercitrin) as well as kaempferol and its glycosides (astragalin), are the main therapeutic constituents in PLE (Bei et al., 2004).

For years, PLE was widely used for the treatment of stroke and apoplexy syndrome in China (Bei et al., 2004), as well as the treatment of hypertensive disease in Japan (Funayama and Hikino, 1979). Currently, pharmacological and clinical studies indicate that PLE, especially its flavonoids, exhibit a wide array of therapeutic activities, such as treating medulloblastoma (Labbe et al., 2009), mucin hypersecretion in airway inflammation (Kwon et al., 2009), atopic dermatitis (Matsumoto et al., 2002), etc. Specifically, quercetin is widely known for its anti-oxidant, anti-inflammatory, anti-cancer, and anti-allergic properties (Gao et al., 2009; Rogerio et al., 2010), and kaempferol has been shown to have protective activity against oxidative stress, which plays a significant role in the onset of Alzheimer's disease (Kim et al., 2010), and exhibits cancer chemo preventive efficacy (Barve et al., 2009). Additionally, other constituents in the PLE such as the triterpenoids (Chen et al., 2002; Thuong et al., 2008), polyphenol (An et al., 2005), betulinic acid 3-caffeate (Ma et al., 2008) and the whole persimmon leaf (Lee et al., 2006) have been reported to exhibit a variety of pharmacological activities.

However, commercially available PLE tablets (Naoxinqing tablets) show low dissolution in water. Consequently, simultaneously improving the solubility of all the components of PLE is the top priority. Of all the constituents, quercetin and kaempferol aglycones are known to possess low bioavailability, specifically 16.2% for quercetin (Khaled et al., 2003) and 1.9% for kaempferol (Barve et al., 2009) in rats. Previous findings have shown that humans absorbed appreciable amounts of quercetin and its absorption may be enhanced by conjugation with glucose (Hollman et al., 1995). Therefore, it is reasonable to infer that PLE, in which quercetin exist as glycoside derivatives, could enhance the absorption of quercetin. Until this point, however, only a few formulation strategies were reported to enhance the oral absorption of PLE further.

The self-emulsifying drug delivery system (SEDDS) has been developed for the purpose of improving solubility, dissolution and oral absorption of poorly water-soluble drugs with a simple one step process. The marketed SEDDS formulations, such as Sandimmune Neoral® (cyclosporin), Norvir® (ritonavir) and Fortovase® (saquinavir), have proved the effectiveness of this drug delivery system. Relatively smaller droplet size would lead to relatively larger interfacial surface area for drug absorption. As a result, SNEDDS has the potential to improve absorption further. SNEDDS

* Corresponding author. Tel.: +86 20 39943118; fax: +86 20 39943118.
E-mail address: zhaocs@mail.sysu.edu.cn (C. Zhao).

0378-5173/$ – see front matter © 2011 Elsevier B.V. All rights reserved.
doi:10.1016/j.ijpharm.2011.08.024

disperses in the gut and forms nanoemulsion under mild agitation of the gastrointestinal tract. It improves the bioavailability partly by keeping the drug in solution in the gut, avoiding the dissolution step (Pouton, 1997). Other mechanisms by which SNEDDS enhances the bioavailability of hydrophobic drugs include the stimulation of pancreatic and biliary secretions, as well as lymphatic transport, prolongation of gastrointestinal residence time, increased intestinal wall permeability, and reduced metabolism and efflux pump activity (Narang et al., 2007). Ease of production and increase stability are also advantages of SNEDDS (Gershanik and Benita, 2000). However, so far the PLE formulated in SNEDDS has not been evaluated for improving the solubility and oral bioavailability.

The objectives of the current study were to design, prepare, characterize and evaluate a stable SNEDDS formulation of PLE. The pseudo-ternary phase diagrams were constructed by a modified PDMPD method, which enabled a more exact status description than the traditional titration method (drop method). The nanoemulsion formulations were optimized by an extreme vertices experiment design. HPLC methods for quantifying PLE *in vitro* and *in vivo* samples were established by detecting the concentrations of the quercetin and kaempferol after hydrolysis of the PLE, which turns the glycosides to aglycones. The relative oral bioavailability of the developed PLE-loaded SNEDDS versus the commercially available PLE tablets was evaluated in beagle dogs.

2. Materials and methods

2.1. Materials

The PLE was supplied by Guilin Sanleng Biotech Co., Ltd. (Guangxi, China). Quercetin and kaempferol were purchased from the National Institute for the Control of the Pharmaceutical and Biological Products (Beijing, China). Naoxinqing tablets (containing 15 mg PLE total flavonoids in one tablet, lot no.: G 8A001) were manufactured by Hutchison Whampoa Guangzhou Baiyunshan Chinese medicine Co. (Guangzhou, China). Labrasol®, Labrafil® M 1944 CS (oleoyl macrogol glyceride), Labrafil® M 2125 CS (linoleoyl macrogol glyceride), Transcutol® P and Maisine® 35-1 were kindly donated by Gattefosse (Saint-Priest Cedex, France). Cremophor® EL was provided by BASF (Ludwigshafen, Germany). All other chemicals and solvents were of reagent grade and used without further purification.

2.2. Solubility studies

Solubility studies were conducted by adding an excess amount of PLE powder to 2 mL of oils, surfactants, co-surfactants or different formulations. The mixtures were then eddied and sonicated for 30 min, respectively, followed by shaking in a 37 °C water bath for 72 h to reach equilibrium. The supersaturated samples were centrifuged at the speed of 16,000 rpm for 10 min to separate the undissolved PLE. The quantification of PLE was based on the determination of quercetin and kaempferol. Since they existed as glycoside derivatives in PLE, the samples were hydrolyzed before determination. The hydrolysis proceeded as follows: about 0.02 g of the supernatant was diluted with 10 g of 37% HCl–methanol (1:4, v/v) solution and hydrolyzed for 1 h in an 80 °C water bath. After the mixture cooled to room temperature, an equivalent weight of methanol was added to compensate for the evaporation loss. All the samples were analyzed by HPLC after filtering through a 0.45 μm membrane filter.

2.3. HPLC method

The HPLC system (Hitachi, Tokyo, Japan) was equipped with two pumps (L-2130), a diode array detector (L-2450), an autosampler (L-2200) and a data station (EZChrom Elite, Hitachi). Samples were separated by Diamonsil-C_{18} column (200 mm × 4.6 mm, 5 μm, Dikma) guarded with a C_{18} precolumn (4 mm × 3.0 mm, Phenomenex). The mobile phase consisting of acidic aqueous solution (0.02% phosphoric acid)–methanol (48:52, v/v) was pumped at a flow rate of 1.0 mL/min. The column eluant was monitored at 360 nm at 40 °C.

2.4. Preparation of SNEDDS for PLE

The PLE was dissolved in surfactant and co-surfactant mixture with frequent shaking, and oil was then added. The mixtures were eddied and sonicated for 20 min, respectively.

2.5. Droplet size analysis and zeta potential

The average droplet size and polydispersity index (PDI) of SNEDDS were measured by photon correlation spectroscopy (PCS) using a Malvern Zetasizer (Nano-ZS90, Malvern Instruments Ltd., UK) with a 50 mV helium–neon laser at the wavelength of 633 nm. The measurements were performed at 25 °C at a scattering angle of 90°. The chosen formulations were diluted by distilled water with a ratio of 1:600 (g/g) and mixed for 1 min using a magnetic stirrer. Zeta potential measurements were carried out on the same diluted sample using the same equipment and operating conditions. The particles' velocity was measured using the technique of laser Doppler anemometry. The zeta potential was determined 20 times for each sample at 25 °C, and the values were calculated according to the Smoluchowski equation.

2.6. Construction of pseudo-ternary phase diagram

The Phase Diagram by Micro Plate Dilution (PDMPD) method, based on the water titration method, is novel for phase diagram construction (Schmidts et al., 2009). In brief, the mixtures of oil, surfactant and co-surfactant (oil-emulsifier phase) at certain weight ratios were gradually diluted with water in a microtitre plate (96 wells, 350 μL volumes each). The microtitre plates were filled by pipette in accordance with the filling scheme: the oil-emulsifier phase was added starting from A_1 with 200 μL, A_2 with 190 μL, continuing to B_8 with 10 μL, decreasing 10 μL each well, and the water phase was then added from A_2 with 10 μL, A_3 with 20 μL, continuing to B_9 with 200 μL, increasing 10 μL each well. The wells C_1 to D_9 were filled with the next batch using the same procedure. The plates were then sealed with their associated lids and eddied for 10 min. As visual evaluation of the border between the homogeneous and the heterogeneous system of the original method was unconvincing, we improved the evaluation method to detect the turbidity of each well by Multiskan Ascent (Thermo Electron Corporation, USA) at 630 nm.

The pseudo-ternary phase diagrams were used to choose surfactant and obtain the concentration range of components for the existing region of nanoemulsion. For choosing surfactant, the ratio of surfactant to co-surfactant (K_m) was fixed at 3:1 (w/w), and the different ratio of oil to the mixture of surfactant and co-surfactant was 1:9, 2:8, 3:7, 4:6, 5:5, 6:4, 7:3, 8:2 and 9:1 (w/w). The concentrations of components were recorded to complete the pseudo-ternary phase diagrams. For obtaining the concentration range, a series of SNEDDS were prepared with varying weight percentages of oil, surfactant and co-surfactant at room temperature. The droplet sizes of the formulations were measured according to the method mentioned in Section 2.5. If the average droplet size was less than 100 nm, the corresponding region in the phase diagram was labeled as grey to describe the self-emulsification region.

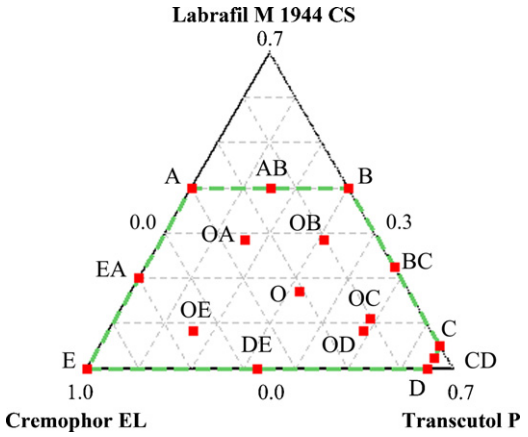

Fig. 1. Extreme vertices mixture design field with boundary limitations (dotted area with the ratio of surfactant was in the range of 30–100%, 0–40% for oil and 0–65% for co-surfactant) and experimental points for a three-component system.

2.7. Formulation optimization of PLE-loaded SNEDDS

The extreme vertices experiment design was used to optimize the composition of SNEDDS. In this design, three factors were evaluated by changing concentrations of components simultaneously and keeping the total concentration constant. The extreme vertices design for a three-component system was represented by an equilateral triangle in two-dimensional space. As the concentration ranges of oil, surfactant and co-surfactant were bounded according to the results mentioned in Section 3.2, the extreme vertices design just covered a part of the equilateral triangle. Sixteen batches of SNEDDS carrying PLE were prepared (Fig. 1), including five vertices (A, B, C, D, E), five halfway points between vertices (AB, BC, CD, DE, EA), one center point (O), and five axial points, midpoints between vertices and center point (OA, OB, OC, OD, OE). The concentrations of oil (X_1), surfactant (X_2) and co-surfactant (X_3) were chosen as the independent variables. The solubility of total PLE flavonoids in SNEDDS (Y_1) and the droplet size of formed nanoemulsion by diluting with distilled water (Y_2) were taken as responses. Further optimization was performed using the desirability function (Liu et al., 2009). In brief, for a response to be minimized, the desirability function was defined as:

$$d_i = \frac{Y_{\max} - Y_i}{Y_{\max} - Y_{\min}} \quad (1)$$

For a response to be maximized, the desirability function was defined as:

$$d_i = \frac{Y_i - Y_{\min}}{Y_{\max} - Y_{\min}} \quad (2)$$

The limits were selected for Y_1: $Y_{max} = 54$ (highest solubility) and $Y_{min} = 18$ (lowest tolerable solubility); Y_2: $Y_{max} = 202.5$ (largest tolerable droplet size) and $Y_{min} = 17.5$ (desired droplet size). Then the overall desirability (D) was calculated as follows:

$$D = (d_1 d_2 \cdots d_k)^{1/k} \quad (3)$$

where k was the number of the responses. The aim was to obtain the condition on the design variables that maximize D.

Graphs of these properties in the form of contour plot were constructed using Minitab 15.0 (Minitab Inc., USA), the same as the design. The responses for sixteen formulations were fitted to a cubic polynomial model. The mathematical models were expressed as follow:

$$Y = b_0 + b_1X_1 + b_2X_2 + b_3X_3 + b_4X_1^2 + b_5X_1X_2 + b_6X_1X_3 + b_7X_2^2 + b_8X_2X_3 + b_9X_3^2 + b_{10}X_1^3 + b_{11}X_1^2X_2 + b_{12}X_1^2X_3 + b_{13}X_2^3 + b_{14}X_2^2X_3 + b_{15}X_2^2X_1 + b_{16}X_3^3 + b_{17}X_3^2X_2 + b_{18}X_3^2X_1 + b_{19}X_1X_2X_3 \quad (4)$$

where X_1, X_2 and X_3 correspond to the studied factors, Y is the measured response, b_0 is an intercept, and b_1–b_{19} are regression coefficients.

With the aid of SAS 9.0 (SAS Institute Inc., USA), the "total subset" variable selection method was used to develop the model equations. F-test, R^2 and the Adjust R^2 were used to evaluate lack of fit within each model and to identify the fitting model.

2.8. In vitro drug release

The dissolution studies were performed to compare the release characteristics of SNEDDS with the marketed tablets (Naoxinqing tablets), according to US Pharmacopeia XXIV dissolution apparatus II. Hard gelatin capsules, freshly filled with PLE-loaded SNEDDS (~0.6 g; equivalent to 27.72 mg PLE total flavonoids) were put into a sinker, loaded with 900 mL simulated gastric fluid (SGF, 0.1 M HCl, enzyme-free) or simulated intestinal fluid (SIF, pH 6.8 phosphate buffer, enzyme-free) at 37 ± 0.5 °C with paddles set at 50 rpm. Samples (5 mL) were withdrawn at intervals of 3, 6, 9, 15, 30, 45, 60, 90, 120, 150 min and replaced with an equal volume of 37 °C fresh media. The samples were filtered through 0.45 μm membrane filters and the total concentrations of PLE flavonoids was analyzed by TU-1901 ultraviolet spectrophotometer (Beijing Purkinje General Instrument Co., Ltd., China) at 360 nm. All dissolution experiments were performed in sextuplicate.

2.9. Stability studies

Accelerated stability studies were conducted to assess chemical and physical stability of the optimized formulation under refrigeration (4 °C), ambient room temperature (20–25 °C) and high temperature (40 °C). Based on the Chinese Pharmacopoeia (2010 version), the stability studies were conducted for 6 months. The stored samples were evaluated every month by appearance, color, PLE total flavonoids content, droplet size and zeta potential of the diluted SNEDDS.

2.10. In vivo study

2.10.1. Bioavailability studies

All experimental procedures were approved and supervised by the Institutional Animal Care and Use Committee of Sun Yat-sen University (Guangzhou, China). Five beagle dogs, weighing approximately 8.5 kg each, were used to conduct experiments at the Laboratory Animal Center of Sun Yat-sen University (Guangzhou, China). Each fasted for 12 h prior to the experiment and received daily basics 5 h after dosing. Bioavailability of PLE-loaded SNEDDS (2 capsules, 22.5 mg PLE total flavonoids each) was compared with the Naoxinqing tablets (3 tablets, 15 mg PLE total flavonoids each). The study was conducted as an open, randomized, crossover design with a one week interval. The beagle dogs were divided randomly into two treatment groups and administered capsules or tablets, followed by 20 mL, of water at a dose of 45 mg PLE total flavonoids on separate occasions. Blood (2 mL) samples were withdrawn from the femoral artery into heparinized tubes at 0, 0.17, 0.33, 0.5, 0.75, 1, 1.5, 2, 3, 4, 6, 8, 10 and 12 h after oral dosing. Blood samples were centrifuged at 5000 rpm for 10 min to separate the plasma, and stored frozen at −20 °C until analysis was performed by the validated HPLC assay method.

2.10.2. Determination of the plasma concentrations of quercetin and kaempferol by HPLC

The flavanoid glycosides of quercetin and kaempferol in PLE were likely to be hydrolyzed to aglycones *in vivo* by the glycosidase, so the plasma samples were completely hydrolyzed first and the concentrations of the two aglycones were measured to represent the PLE concentration. The HPLC/UV method for simultaneous determination of quercetin and kaempferol in plasma was established in this study. The process was as follows: frozen plasma samples were thawed to room temperature just prior to extraction procedure and thoroughly agitated. 0.4 mL of plasma was added to 40 μL of internal standard (isorhamnetin, 45.54 μg/mL in methanol) and mixed for 30 s. After adding 140 μL of hydrochloric acid (25%, v/v) and eddying for 1 min, the plasma samples were hydrolyzed for 30 min in 80 °C water bath. Then 100 μL of NaOH (6 mol/L) was added to neutralize the excess acid and eddied for 1 min. Extraction of PLE was accomplished by adding 3.6 mL of ethyl acetate–isopropanol (95:5, v/v) and eddying for 5 min. The mixture was then centrifuged at 13,000 rpm for 3 min, after which 3.2 mL of organic layer were transferred to a conical glass tube and evaporated under a light stream of nitrogen at 37 °C. The residue was reconstituted with 100 μL of methanol, eddied for 5 min and centrifuged at 16,000 rpm for 5 min. The supernatant solution was transferred to autosampler vials, and an aliquot of 20 μL was injected into the HPLC system.

2.11. Statistical analysis

The pharmacokinetic parameters were established by a two compartment model analysis using 3p97 pharmacokinetic software (Mathematical Pharmacology Professional Committee of China, China). Maximum plasma concentrations (C_{max}) and time (T_{max}) were observed from the concentration–time data, and the area under the concentration–time curve ($AUC_{0-12\,h}$) was calculated by non-compartmental analysis of the final measurable sample. The relative bioavailability (BA) of the SNEDDS formulation compared to the commercial tablets was calculated using the following equation:

$$\text{Relative BA}\,(\%) = \frac{AUC_{SNEDDS}}{AUC_{TABLET}} \times 100\% \quad (5)$$

Data were presented as means ± S.D. and, where applicable, the differences between the two formulations were analyzed by the paired Student's *t*-test using SPSS 13.0 (SPSS Inc., USA). A *P*-value of less than 0.05 was considered as statistically significant. An analysis of variance (ANOVA) was referred to where necessary.

2.12. In vitro–in vivo correlations

Level A of *In Vitro/In Vivo* Correlations (IVIVC) and nonlinear *In Vitro/In Vivo* Relationships (IVIVR) were studied. The *in vivo* absorption fraction, generated by the Wagner–Nelson method, was plotted versus the *in vitro* dissolution rate in SGF (0.1 M HCl) at the same time points. The data within 2 h were chosen for plotting. The least square method was used to estimate the linear correlations. And the quadratic equation was used to estimate the nonlinear relationships:

$$Y = b_0 + b_1X + b_2X^2 \quad (6)$$

where b_0, b_1, b_2 represent regression parameters associated with each function, Y was *in vivo* absorption fraction and X was the *in vitro* dissolution rate.

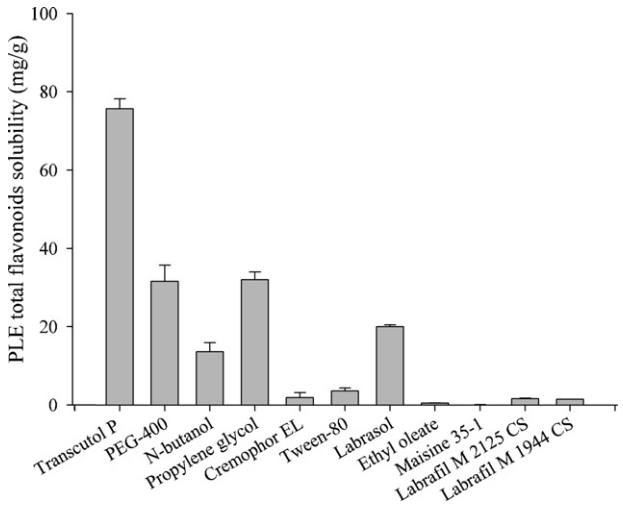

Fig. 2. Solubility study of PLE total flavonoids in various vehicles. Each value represents the mean ± S.D. ($n = 3$).

The following equation was derived assuming first-order dissolution and permeation after oral drug administration (Polli et al., 1996):

$$F_a = \frac{1}{f_a}\left[1 - \frac{\alpha}{\alpha - 1}(1 - F_d) + \frac{1}{\alpha - 1}(1 - F_d)^{\alpha}\right] \quad (7)$$

F_a is the fraction of the total amount of drug absorbed to time t after a single oral dose, f_a is the fraction of the dose absorbed at $t = \infty$, α is the ratio of the first-order permeation rate constant to the first-order dissolution rate constant, and F_d is the fraction of dose dissolved *in vitro* at time t. This equation was examined in order to pursue a theoretical treatment of *in vitro–in vivo* correlation. This equation was examined in order to pursue a theoretical treatment of *in vitro–in vivo* correlation. The values for F_a were obtained by the Wagner–Nelson method; and of F_d were available directly; while the value of f_a was set as the relative AUC. The values for α were calculated both for the SNEDDS and tablet formulations.

As only two dosage forms were researched in current study, Level B and C IVIVC could not be established.

3. Results and discussion

3.1. Solubility studies

The concentrations of PLE total flavonoids in various vehicles were presented in Fig. 2. Among the vehicles tested, Transcutol P (HLB 4.2) which exhibited the highest solubility of total PLE flavonoids (75.67 ± 2.56 mg/mL) was chosen as co-surfactant. The solubility of total PLE flavonoids was similar in Labrafil M 1944 CS and Labrafil M 2125 CS (HLB 4). Labrafil M 1944 CS was chosen for its higher hydrophilic nature than Labrafil M 2125 CS. Due to its emulsion forming capability, Cremophor EL (HLB 12–14) was used as surfactant, although Labrasol (HLB 14) had showed the highest total PLE flavonoids solubility (20.03 ± 0.49 mg/mL) of the surfactants.

3.2. Construction of pseudo-ternary phase diagrams

The components and their concentration ranges were obtained by construction of pseudo-ternary phase diagrams. Labrasol was initially considered as the surfactant, but the mixtures of Labrasol, Transcutol P and Labrafil M 1944 CS were not able to self-emulsify or else yielded unstable emulsions after diluting with distilled water. The surfactants were chosen by pseudo-ternary phase diagram with K_m fixed to 3:1. The PDMPD method was adopted due

to higher precision and speed than the droplet method. Instead of visual evaluation, Multiskan Ascent was used to give evaluation method credibility. When the well turned turbid, the absorbance would increase sharply. Therefore, sudden change of absorbance was the indicator of nanoemulsion and the coarse emulsion. Visual evaluation and image evaluation by scanning the underside of the microtitre plate were used as reference. As showed in Fig. 3, the self-nanoemulsion region of Cremophor EL was larger than that of Labrasol and Tween 80. This may be due to the 18-carbon fatty acid of both Cremophor EL and Labrafil M 1944 CS, which could help Cremophor EL insert into the oil drop surface uniformly. In addition, the polyethylene glycol structure in both of them could bind together through noncovalent interactions such as hydrogen bonding, which made the combination of Cremophor and Labrafil M 1944 CS much tighter. Transcutol P has similar diethylene glycol structure, which could bind with their polyethylene glycol structures to stabilize the nanoemulsion further. The structures of Cremophor EL, Labrafil M 1944 CS and Transcutol P were so similar that they had very good compatibility, predicting a stable nanoemulsion could be obtained. As Labrasol was an 8–10 carbon fatty acid, and Tween 80 had no polyethylene glycol structure, they could not emulsify with Labrafil M 1944 CS and Transcutol P as effectively as Cremophor EL. Therefore, Cremophor EL, Labrafil M 1944 CS and Transcutol P were the best components for nanoemulsion.

After choosing the surfactant, the appropriate concentration ranges of Cremophor EL, Transcutol P and Labrafil M 1944 CS were obtained by constructing phase diagrams. As showed in Fig. 4, the efficiency of emulsification was good when the emulsifier phase concentration was more than 60%, especially when it composed more than 80% of SNEDDS formulation. This demonstrated that the emulsification with less than 30% of surfactant ratio was not efficient. With the increase of co-surfactant, the spontaneity of the self-emulsification process also increased. But when the concentration of the co-surfactant was too high, the PLE would precipitate after diluting with distilled water. Based on these observations, the ratio of surfactant was 30–100%, oil was 0–40% and co-surfactant was 0–65%.

3.3. Formulation optimization

Extreme vertices method was used to optimize the components ratios of the SNEDDS formulation based on the components ratio range mentioned above. Results were reported in Table 1, and the contour plots were further modified to obtain proper formulation (Fig. 5). The three responses were separately fitted to a cubic polynomial model, and then optimized by the "total subset" variable selection method. The model with the highest R^2 was identified as the fitting model (Table 2).

3.3.1. Influence of formulation composition on PLE total flavonoids solubility

SNEDDS formulations are supposed to have good drug solubility. From the levels of significance for regression coefficients in Table 2, oil ratio contributed to the regression model. As showed in Fig. 5(a), increase in oil ratio led to decrease of solubility with other elements fixed. This finding was consistent with the previous study, which demonstrated that the sequence of solubility of total PLE flavonoids was Labrafil M 1944 CS < Cremophor EL < Transcutol P. Therefore, it was reasonable to infer that the content of Transcutol P may be largely responsible for the solubilizing capability of the SNEDDS, and PLE may mainly dissolve in the emulsifying membrane layer formed by surfactant and co-surfactant. When the ratio of oil decreased, the droplet size decreased and the total surface area of the emulsifying membrane layer increased. As a result, the solubilities of PLE total flavonoids increased.

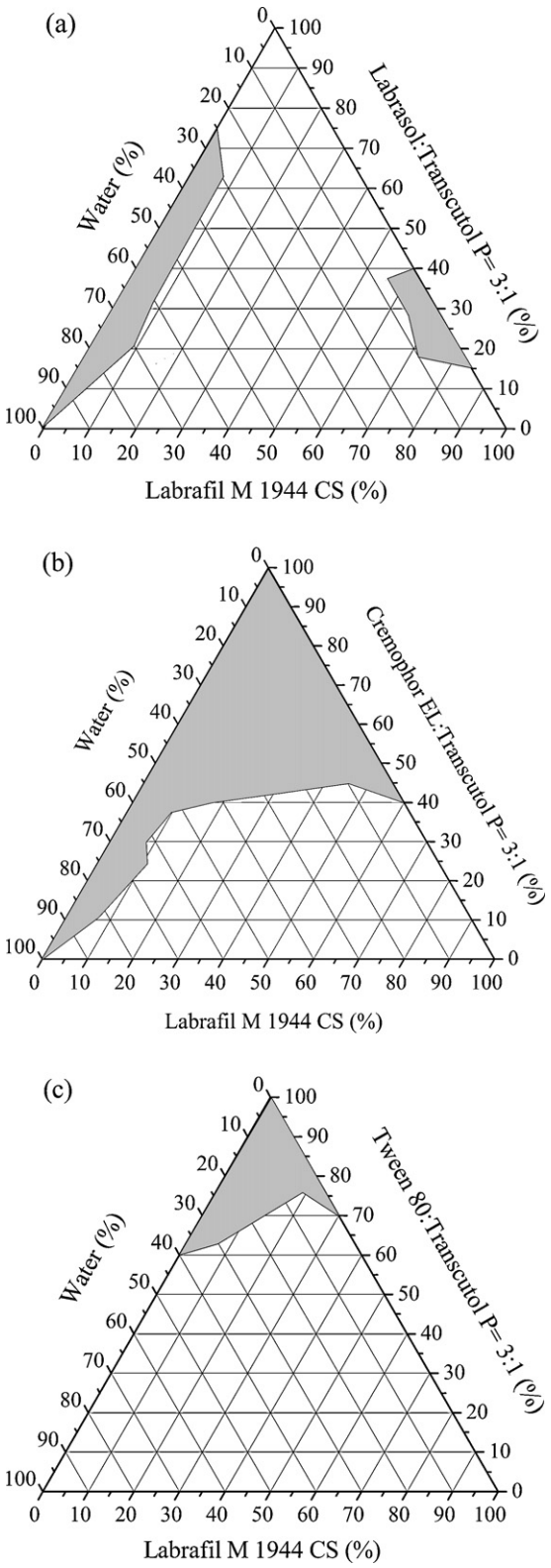

Fig. 3. Pseudo-ternary phase diagram of the formulations composed of various surfactants, Labrasol (a), Cremophor EL (b), Tween 80 (c), using PDMPD method after 24 h without drug. The shadow area represents nanoemulsion region.

3.3.2. Influence of formulation composition on the droplet size

Droplet size was important for assessing SNEDDS. Smaller droplet size provided a larger interfacial surface area for drug absorption. From examining the plots and equations, it was convincing that the droplet size of PLE was related to the ratios of

Table 1
Compositions of sixteen formulations of the extreme vertices design and results (mean ± S.D.; $n = 3$).

Formulation number	Formulation components (%)			Solubility (mg/g)	Droplet size (nm)	D
	Surfactant	Co-surfactant	Oil			
1	0.200	0.800	0.000	20.948 ± 0.069	18.9	0.285
2	0.285	0.555	0.160	33.159 ± 0.071	25.6	0.635
3	0.285	0.405	0.310	29.242 ± 0.003	39.3	0.525
4	0.400	0.600	0.000	18.240 ± 0.026	26.3	0.080
5	0.000	0.675	0.325	49.526 ± 0.096	66.6	0.802
6	0.085	0.430	0.485	49.239 ± 0.086	69.1	0.791
7	0.110	0.405	0.485	50.521 ± 0.037	80.3	0.772
8	0.050	0.300	0.650	50.187 ± 0.078	187.0	0.274
9	0.400	0.300	0.300	21.841 ± 0.022	164.0	0.149
10	0.085	0.755	0.160	38.876 ± 0.019	17.8	0.761
11	0.400	0.450	0.150	25.374 ± 0.344	33.0	0.439
12	0.170	0.510	0.320	45.656 ± 0.059	35.1	0.834
13	0.225	0.300	0.475	26.352 ± 0.025	163.0	0.223
14	0.000	0.350	0.650	51.359 ± 0.029	194.0	0.206
15	0.025	0.325	0.650	53.842 ± 0.037	202.0	0.052
16	0.000	1.000	0.000	38.288 ± 0.040	28.3	0.728

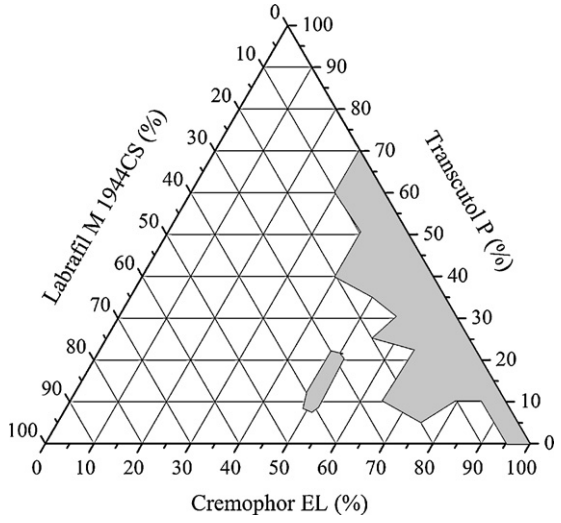

Fig. 4. Pseudo-ternary phase diagram of SNEDDS formulation composed of Labrafil M 1944 CS as oil, Cremopher EL as surfactant and Transcutol P as co-surfactant. The shadow area represents nanoemulsion region.

Table 2
Regression coefficients and statistical analysis.

	Variable	Parameter estimate	P-value	ANOVA
D	Intercept	−3.438	< 0.001	$F = 25.72$, $P < 0.0001$
	Oil content	6.925	0.001	$R^2 = 0.958$
	Sur content	16.924	< 0.001	Adj $R^2 = 0.920$
	(Oil content)^2	−27.607	0.010	
	(Sur content)^2	−30.131	< 0.001	
	(Oil content)^3	33.740	0.037	
	(Sur content)^3	17.374	< 0.001	
	Sur^2 × Co-s	8.059	< 0.001	
Y_1	Intercept	56.398	< 0.001	$F = 38.24$, $P < 0.0001$
	Oil content	−391.182	0.001	$R^2 = 0.971$
	Oil × Sur	1309.525	0.002	Adj $R^2 = 0.946$
	(Sur content)^2	−1048.036	0.002	
	(Oil content)^3	694.834	0.020	
	(Oil)^2 × Sur	−900.320	0.019	
	(Sur content)^3	1029.344	0.002	
	(Sur)^2 × Co-s	1032.932	0.001	
Y_2	Intercept	23.831	0.0084	$F = 86.08$, $P < 0.0001$
	Co-s content	814.183	0.0004	$R^2 = 0.977$
	Sur × Co-s	−5121.547	< 0.0001	Adj $R^2 = 0.966$
	(Oil)^2 × Co-s	3039.078	0.0003	
	(Sur)^2 × Co-s	4696.433	< 0.0001	
	(Co-s)^2 × Sur	2900.913	0.0004	

surfactant and co-surfactant. As shown in Fig. 5(b), the droplet size had an enlarging trend on the whole when the ratio of co-surfactant was increased. In addition, variables including Sur × Co-s, (Sur)^2 × Co-s, (Co-s)^2 × Sur were also significant (as shown in Table 2). It was inferred that the interaction of surfactant and co-surfactant played an important role in droplet size of SNEDDS.

3.3.3. Optimization by desirability function

The solubility (Y_1) and droplet size (Y_2) responses were transformed into the desirability scales d_1, d_2, respectively. Y_1 had to be maximized, while Y_2 had to be minimized. The overall objective function (D) was calculated by Eq. (3) and the result is shown in Table 1. The model was also fitted with a cubic polynomial model and optimized by the "total subset" variable selection method using SAS 9.0 (SAS Institute Inc., USA), and the regression equation is

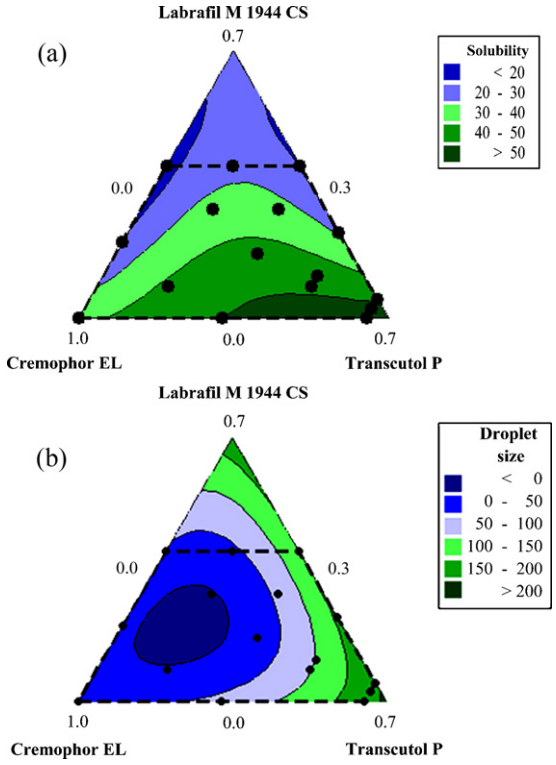

Fig. 5. The contour plots of response: solubility (a) and droplet size (b).

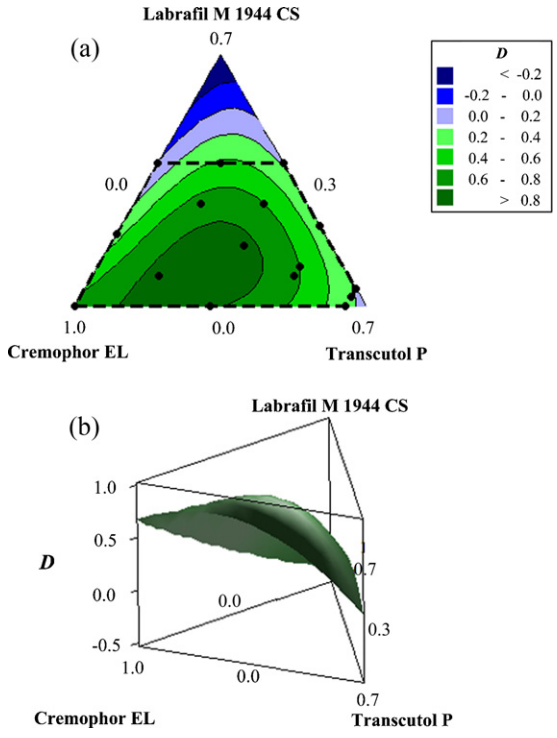

Fig. 6. The contour plots (a) and surface plots (b) of overall desirability (*D*).

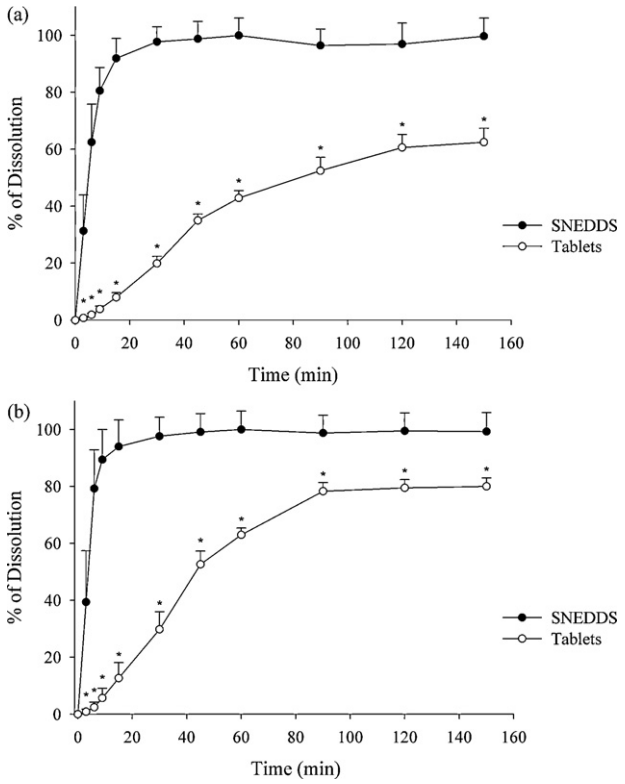

Fig. 7. PLE release profile from (●) SNEDDS and (○) conventional tablets in SGF (a) and SIF (b). Each value represents the mean ± S.D. ($n = 6$). *Significantly different ($P < 0.05$) compared the SNEDDS with the conventional tablets by the unpaired Student's *t*-test at the same time point.

shown in Table 2. Fig. 6 showed the response surface for *D*, and the darkest green domain at Fig. 6(a) is the optimization region. After calculating with step width of 0.1, the maximum function value was obtained at X_1: 0.1, X_2: 0.56, X_3: 0.34. To confirm the model adequacy for prediction, three batches of formulations under the optimum composition were prepared. As the results shown in Table 3 demonstrate, the model was validated due to close agreement between the predicted and experimental results, and the optimal formulation of PLE-loaded SNEDDS was: Labrafil M 1944 CS: 10%, Cremophor EL: 56% and Transcutol P: 34%.

3.4. SNEDDS characterization

The parameters for physicochemical characteristics of the optimized formulation with or without PLE after dilution with distilled water are shown in Table 4. Droplets size was slightly increased by the incorporation of PLE in the SNEDDS system, which may be because that PLE mainly dissolved in the emulsifying membrane layer (formed by surfactant and co-surfactant). Additionally, the PLE exhibited acidity, which made the pH lower and the zeta potential higher than the blank formulation.

3.5. In vitro drug release

The conventional *in vitro* release method with pH change was chosen because recent study indicates that the formulation of micelles inside the dialysis bag was delayed or disturbed, and the paddle method gave valuable information about the dispersion and the solubilization ability of the SNEDDS formulation at different pH values over time (Do Thi et al., 2009). The results are shown in Fig. 7.

The total PLE flavonoids released from the SNEDDS were significantly greater and faster than the marketed tablets ($P < 0.05$). Both in SIF and SGF, the SNEDDS released more than 80% in 9 min at 37 °C, while the marketed tablets released 3.88% in SIF and 5.70% in SGF. The total PLE flavonoids dissolution percentages of the tablets in SIF (80.02%) were significantly higher than those in SGF (62.46%, $P < 0.001$). This may be because the phenolic hydroxyl groups of the flavonoids exhibited acidity, which made the PLE dissolve more readily at higher pH. However, the dissolution of the SNEDDS did not show significant difference between SIF (99.69%) and SGF (99.26%, $P = 0.488$). A possible explanation was that most of the drug in the SNEDDS solution did not exist in free molecular form as the tablets. They were entrapped in the nanoemulsion droplets, or in the interface formed by the surfactant and co-surfactant. As the phenolic hydroxyl groups of the flavonoids were not exposed to the media, the pH of the media did not produce any effect. This also proves that the flavonoids of the PLE were solubilized by nanoemulsion. Ultimately, the total dissolutions of the tablets were limited by the poor solubility of PLE total flavonoids in aqueous media. By comparison, the SNEDDS completely dissolved in 9 min without pH influence. This shows that the total PLE flavonoids in SNEDDS could dissolve and consequently be absorbed more rapidly and completely than the tablets in the stomach or intestine. Thus, improvement of PLE bioavailability could be anticipated.

Table 3
The predicted values and the experimental results of PLE-loaded SNEDDS prepared under the optimum conditions.

Response	Predicted value	Experimental value	Bias (%)
Y_1, solubility (mg/mL)	48.70	44.48	−8.67
Y_2, droplet size (nm)	24.94	34.85	39.74

Bias (%) = (predicted value − experimental value)/experimental value × 100.

3.6. Stability studies

During the 6 months of stability studies, none of the SNEDDS samples showed any change in color or appearance under all

Table 4
Physicochemical parameters of the optimized SNEDDS after diluted by distilled water.

Samples	Mean droplet size (nm)	PDI	Zeta potential (mV)	pH
Blank SNEDDS	17.68 ± 1.30	0.19 ± 0.05	−25.54 ± 9.08	5.93 ± 0.08
PLE-loaded SNEDDS	34.85 ± 17.10	0.23 ± 0.02	−6.18 ± 1.17	4.10 ± 0.02

storage conditions. The total PLE flavonoids content of the SNEDDS was stable for at least 6 months at 40 °C, 25 °C and 4 °C. No significant differences were found in droplet size or zeta potential at zero time through the 6 months stability study period under all storage conditions by one-way ANOVA test. This suggested that PLE-loaded SNEDDS was stable under above conditions.

3.7. *In vivo* study

In plasma extracts, quercetin, kaempferol and internal standard isorhamnetin were well purified by HPLC (Fig. 8). The linearity of the calibration curves were in the range of 0.075–10.0 μg/mL (R^2 = 0.9994) for quercetin and 0.005–2.0 μg/mL (R^2 = 0.9975) for kaempferol in plasma. At concentrations of 0.075, 0.25 and 0.5 μg/mL, recoveries of quercetin from dog plasma extracts were 98.91%, 108.83%, and 111.77%. Inter-day precisions were 8.01%, 4.20%, and 7.86%, and intra-day precisions were 9.27%, 10.53%, and 7.32%. At concentrations of 0.005, 0.05 and 0.1 μg/mL, recoveries of kaempferol from dog plasma extracts were 94.00%, 88.01%, and 90.68%. Inter-day precisions were 14.63%, 6.97%, and 7.61%, and intra-day precisions were 12.30%, 11.07%, and 8.00%. After storage at room temperature for 12 h and freeze-thawing three times, quercetin, kaempferol and internal standard isorhamnetin were stable in plasma.

The *in vivo* study was performed to quantify quercetin and kaempferol plasma concentrations after oral administration of PLE. Fig. 9 shows the mean plasma concentration versus time profiles of quercetin and kaempferol for PLE-loaded SNEDDS and conventional tablets following oral administration in a total of five beagle dogs. The pharmacokinetic parameters of PLE were computed according to the method mentioned in Section 2.11 and the results are tabulated in Table 5. The SNEDDS gave significantly higher AUC, C_{max}, and K_a than conventional tablets ($P < 0.05$). In particular, for the quercetin and kaempferol of SNEDDS, the $AUC_{0-12\,h}$ was 1.5-fold and 1.6-fold greater respectively than conventional tablets, the C_{max} was 1.6-fold and 1.3-fold greater, and the K_a was 1.7-fold and 1.9-fold greater. This demonstrates that the PLE of SNEDDS could be absorbed more and faster and in greater concentration than conventional tablets. It further demonstrated that the enhancement of solubility and *in vitro* dissolution of PLE in SNEDDS could increases the GI absorption of PLE after oral administration in beagle dogs. However, as the value of T_{max} from tablets was low already and all of the values of T_{max} were varied widely between individuals, the time for SNEDDS to reach peak concentration was shorter than the conventional tablets, but not in a significant way. The difference of MRT was also insignificant. This may be because the SNEDDS did not change from the *in vivo* distribution pattern seen in the tablets. As a result, the residence time of PLE *in vivo* is unchanged.

An aspect of note in the concentration–time profiles was the two observed peaks in both the quercetin and kaempferol profiles, which may be due to the entero-hepatic biliary recycling of both. Another possible explanation is that the second peaks around 6–10 h were due to delayed absorption of quercetin and kaempferol in the jejunum and ileum through lymphatic transport. According to the triple-cannulated canine model, Holm determined the drug concentration of plasma and lymph, and then proved that the lymphatic transport played a major role in the absorption of the SMEDDS from the intestine (Holm et al., 2003). It is possible that

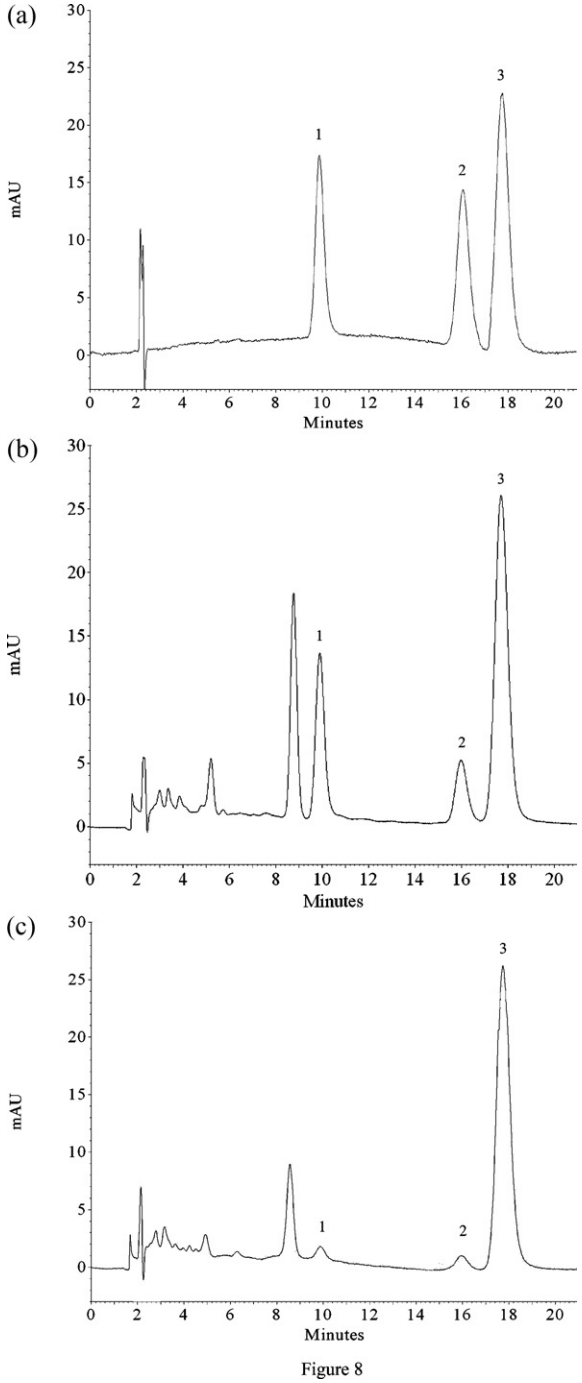

Fig. 8. Representative chromatograms of mixed standard preparations: (a) *in vitro* mixed standard; (b) mixed standard added to blank plasma; (c) plasma samples of beagle dogs. (Key: peak 1 was quercetin, 2 was kaempferol, 3 was internal standard isorhamnetin.)

Table 5
Pharmacokinetic parameters of SNEDDS and Conventional tablets following oral administered to fasted beagle dogs. Each value represents the mean ± S.D. ($n = 5$).

Parameter	SNEDDS		Conventional tablets	
	Quercetin	Kaempferol	Quercetin	Kaempferol
$AUC_{0\to 12\,h}$ (μg h/mL)	1.94 ± 0.67*	0.58 ± 0.12*	1.31 ± 0.18	0.36 ± 0.08
C_{max} (μg/mL)	0.34 ± 0.06*	0.10 ± 0.04*	0.21 ± 0.04	0.08 ± 0.01
T_{max} (h)	1.50 ± 0.50	1.60 ± 0.42	1.90 ± 0.74	2.05 ± 0.97
K_a (h^{-1})	5.26 ± 1.90*	6.28 ± 1.62*	2.89 ± 0.27	2.81 ± 0.39
K_{10} (h^{-1})	0.45 ± 0.09	0.37 ± 0.09	0.38 ± 0.06	0.59 ± 0.23
K_{12} (h^{-1})	0.15 ± 0.04	0.18 ± 0.10	0.20 ± 0.06	0.28 ± 0.13
K_{21} (h^{-1})	0.62 ± 0.13	0.59 ± 0.11	0.62 ± 0.15	0.52 ± 0.18
$T_{1/2\alpha}$ (h)	0.78 ± 0.18	0.80 ± 0.15	0.74 ± 0.15	0.67 ± 0.24
$T_{1/2\beta}$ (h)	2.40 ± 0.62	2.92 ± 0.53	2.89 ± 0.07	2.87 ± 0.73
$MRT_{0\to 12\,h}$ (h)	4.52 ± 0.56	5.08 ± 0.47	4.45 ± 0.56	4.74 ± 0.96

* $P < 0.05$ compared with conventional tablets.

the same is true in the SNEDDS. The beagle dogs were fed 5 h after dosing which may help the absorption in the jejunum and ileum. The concentration of bile salt would increase after food intake, especially the concentrations of its lipid. Bile salts may decrease duodenal and jejunal brush-border membrane vesicle integrity, increase membrane fluidity and passive proton permeability (Zhao and Hirst, 1990), which might increase the absorption of quercetin and kaempferol in the gut. While both the SNEDDS and the tablets had elevated plasma concentrations, the peaks of the SNEDDS were much higher and lasted longer. This may be because the lipids in the SNEDDS, in conjunction with the lipids in food, triggered the biochemical processes involved in the lymphatic transport of lipids. The lipid, especially the long-chain fatty acids in the SNEDDS, may have been re-esterified to triglycerides within the intestinal cell, incorporated into chylomicrons and secreted from the intestinal cell by exocytosis into the lymph vessels (Holm et al., 2003). Therefore, the SNEDDS may transport more drugs by intestinal lymphatics than the tablets, and last longer as the tablets depended on the little lipid in normal food and the endogenously derived lipid. The second peaks in the kaempferol profiles seemed higher than the quercetin. This may be due to the first peaks of the kaempferol were lower than the quercetin, making the second peaks seem more significant. Another reason may be that the hydroxyls in the kaempferol are less than quercetin. Additional lipophilic properties helped kaempferol bind more tightly to the lipid, and promoted its lymphatic transport.

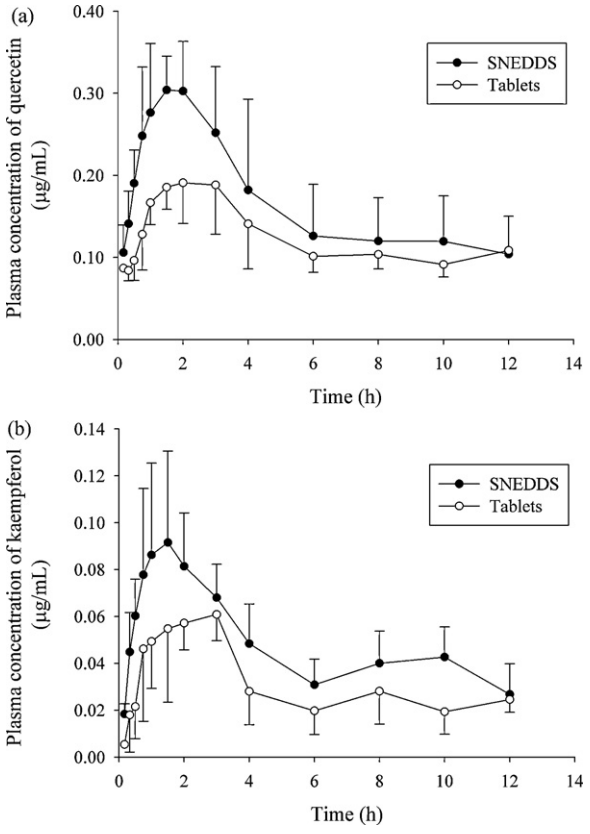

Fig. 9. Mean quercetin (a) and kaempferol (b) plasma concentration–time profile ± S.D. following oral administration of (●) SNEDDS or (○) conventional tablets to beagle dogs ($n = 5$).

For a poorly water-soluble drug, its absorption is often limited by the insufficient dissolution in the gastrointestinal tract (Zhang et al., 2008). Therefore, the dissolution process might be a critical factor influencing the adsorption. During the *in vitro* study, the disintegration of the conventional tablets promoted the drug dispersion, but some of the PLE powder agglomerated. The final dissolution was still constrained by the poor water solubility of flavonoids in the PLE. The SNEDDS spontaneously formed nanoemulsion, presenting the drug in its dissolved state. This sped up the process of drug absorption and ensured that the drug would not agglomerate or precipitate in the GI tract. The small droplets of the nanoemulsion with drugs could pass through the membrane directly and be absorbed easier (de Smidt et al., 2004).

Another reason the SNEDDS improved oral delivery was that it improved lymphatic absorption. The quercetin microemulsion was found to be absorbed mainly in the colon and ileum, and abounded in the collecting lymphatic vessel (Gao et al., 2009). Nanoemulsion had a tendency to adhere to collecting lymphatic vessel surface and transferred via M cell, so the lymphatic absorption was an important absorption route for the PLE-loaded SNEDDS. It has been shown that more quercetin in the microemulsion can be absorbed faster in rat intestine than in micelle solution due to the enhancement of the lymphatic absorption by the lipid (Gao et al., 2009). Therefore, the oil phase might be the key point to the lymphatic absorption. The long-chain oil, Labrafil M 1944 CS chosen here gave a positive effect. Relative to medium chain glycerides, long chain glycerides can facilitate lymphatic absorption for highly lipophilic compounds more effectively in dogs (Khoo et al., 2003). The digestion products of long-chain triglycerides were preferentially resynthesized in the enterocyte, assembled into lipoproteins, and secreted into the mesenteric lymph, whereas medium chain triglycerides were primarily absorbed directly into the portal blood (Balakrishnan et al., 2009).

The main rate-limiting barrier for quercetin absorption is the layer of intestinal epithelial cell (Gao et al., 2009). The exogenous surfactants in the formulation reversiblely increase drug permeability by disrupting the lipid bilayer of the epithelial cell membrane (Gursoy and Benita, 2004). Surfactant monomers are capable of embedding in the cell membrane where they can form

Table 6
The nonlinear *In Vitro/In Vivo* Relationships of SNEDDS and conventional tablets.

	Formulation	Equation	R^2
Linear IVIVC			
Quercetin	Tablet	$Y = 0.62X + 0.09$	0.9438
	SNEDDS	$Y = 1.85X - 1.41$	0.6231
Kaempferol	Tablet	$Y = 0.95X + 0.02$	0.9860
	SNEDDS	$Y = 2.43X - 1.91$	0.7893
Nonlinear IVIVR			
Quercetin	Tablet	$Y = 0.96X^2 + 0.06X + 0.16$	0.9928
	SNEDDS	$Y = 21.96X^2 - 37.93X + 16.44$	0.8255
Kaempferol	Tablet	$Y = 0.11X^2 + 0.92X + 0.03$	0.9860
	SNEDDS	$Y = 20.23X^2 - 34.07X + 14.42$	0.9108

polar defects in the lipid bilayer. At high surfactant concentrations in the cell membrane, surfactant–surfactant contact occurs, and the membrane can be dissolved into surfactant–membrane mixed micelles (Swenson and Curatolo, 1992). Surfactant also demonstrated a reversible effect on the opening of tight junction; it may interact with the polar head groups of the lipid bilayers, modifying hydrogen bonding and ionic forces between these groups. It may also insert itself between the lipophilic tails of the bilayers, resulting in a disruption of the lipid-packing arrangement (Wu et al., 2006).

In the present investigation, the formation of nano-size emulsion, the high content of surfactant and the long-chain fatty acid might all contribute to the increased bioavailability of PLE after oral administration.

3.8. *In vitro–in vivo correlation development*

Linear IVIVC were established. All the dissolution data of the control (tablets) correlated with the *in vivo* data (shown in Table 6). However, the data of SNEDDS did not exhibit significant correlation. Then, the nonlinear IVIVR were established and all the data of the tablets and SNEDDS correlated well. In current study, for quercetin and kaempferol of SNEDDS, α were 0.00238 and 0.00260, respectively; of tablets, α were 0.362 and 0.205, respectively. It indicated that the release rate of drugs in SNEDDS and tablets were higher than the absorption rate *in vivo*, especially for SNEDDS. In other words, both of them were permeation-rate-limited. As a result, neither of them could meet the criteria for a USP Level A correlation. Values for α of tablets were nearly 100-fold more than SNEDDS. This maybe because that the SNEDDS could increase the dissolution rate k_d markedly. As the permeation process is passive diffusion process, the passive diffusion rate k_d is determined by the drug concentration and diffusion area. The SNEDDS could release much faster than the tablets, which could increase the drug concentration markedly. And the SNEDDS could form nanoemulsion in gastrointestinal tract and greatly increase the absorption area. As a result, the increase of drug concentration in gastrointestinal tract and absorption area finally significantly increased the AUC and k_a of SNEDDS, which were proved by the *in vivo* study.

4. Conclusions

The PLE was successfully formulated as a stable SNEDDS formulation that had significant improvement in solubility, *in vitro* release and bioavailability compared with commercially available tablets. An optimized formulation of SNEDDS was developed by the extreme vertices mixture design. Dissolution of total PLE flavonoids in SNEDDS in pH 1.2 and 6.8 buffer solution was significantly faster and released more flavonoids than commercial tablets. The oral bioavailability of quercetin and kaempferol *in vivo* in beagle dogs was significantly enhanced by SNEDDS compared with commercial tablets. According to the *in vitro–in vivo* correlation study, the oral bioavailability enhancement was due to the increase of drug concentration in GI tract and absorption area. Overall, the studies show that it is promising to produce stable SNEDDS via a simple one-step process for poorly aqueous soluble drugs, including the extract of Chinese herbal medicine, to achieve a significant improvement in the bioavailability.

Acknowledgments

We gratefully thank Andrew Spangle M.D. from School of Medicine University of North Carolina at Chapel Hill, for his kindness in carefully revising the language of this article. We acknowledge financial support from Department of Science and Technology, Guangdong, P.R. China (Grant 2006B35604007).

References

An, B.J., Kwak, J.H., Park, J.M., Lee, J.Y., Park, T.S., Lee, J.T., Son, J.H., Jo, C., Byun, M.W., 2005. Inhibition of enzyme activities and the antiwrinkle effect of polyphenol isolated from the persimmon leaf (*Diospyros kaki folium*) on human skin. Dermatol. Surg. 31, 848–854.

Balakrishnan, P., Lee, B.J., Oh, D.H., Kim, J.O., Lee, Y.I., Kim, D.D., Jee, J.P., Lee, Y.B., Woo, J.S., Yong, C.S., Choi, H.G., 2009. Enhanced oral bioavailability of Coenzyme Q(10) by self-emulsifying drug delivery systems. Int. J. Pharm. 374, 66–72.

Barve, A., Chen, C., Hebbar, V., Desiderio, J., Saw, C.L., Kong, A.N., 2009. Metabolism, oral bioavailability and pharmacokinetics of chemopreventive kaempferol in rats. Biopharm. Drug Dispos. 30, 356–365.

Bei, W.J., Peng, W.L., Ma, Y., Xu, A.L., 2004. NaoXinQing, an anti-stroke herbal medicine, reduces hydrogen peroxide-induced injury in NG108-15 cells. Neurosci. Lett. 363, 262–265.

Chen, G., Lu, H., Wang, C., Yamashita, K., Manabe, M., Xu, S., Kodama, H., 2002. Effect of five triterpenoid compounds isolated from leaves of *Diospyros kaki* on stimulus-induced superoxide generation and tyrosyl phosphorylation in human polymorphonuclear leukocytes. Clin. Chim. Acta 320, 11–16.

de Smidt, P.C., Campanero, M.A., Troconiz, I.F., 2004. Intestinal absorption of penclomedine from lipid vehicles in the conscious rat: contribution of emulsification versus digestibility. Int. J. Pharm. 270, 109–118.

Do Thi, T., Van Speybroeck, M., Barillaro, V., Martens, J., Annaert, P., Augustijns, P., Van Humbeeck, J., Vermant, J., Van den Mooter, G., 2009. Formulate-ability of ten compounds with different physicochemical profiles in SMEDDS. Eur. J. Pharm. Sci. 38, 479–488.

Funayama, S., Hikino, H., 1979. Hypotensive principles of *Diospyros kaki leaves*. Chem. Pharm. Bull. (Tokyo) 27, 2865–2868.

Gao, Y., Wang, Y., Ma, Y., Yu, A., Cai, F., Shao, W., Zhai, G., 2009. Formulation optimization and in situ absorption in rat intestinal tract of quercetin-loaded microemulsion. Colloids Surf. B: Biointerfaces 71, 306–314.

Gershanik, T., Benita, S., 2000. Self-dispersing lipid formulations for improving oral absorption of lipophilic drugs. Eur. J. Pharm. Biopharm. 50, 179–188.

Gursoy, R.N., Benita, S., 2004. Self-emulsifying drug delivery systems (SEDDS) for improved oral delivery of lipophilic drugs. Biomed. Pharmacother. 58, 173–182.

Hollman, P.C., de Vries, J.H., van Leeuwen, S.D., Mengelers, M.J., Katan, M.B., 1995. Absorption of dietary quercetin glycosides and quercetin in healthy ileostomy volunteers. Am. J. Clin. Nutr. 62, 1276–1282.

Holm, R., Porter, C.J., Edwards, G.A., Mullertz, A., Kristensen, H.G., Charman, W.N., 2003. Examination of oral absorption and lymphatic transport of halofantrine in a triple-cannulated canine model after administration in self-microemulsifying drug delivery systems (SMEDDS) containing structured triglycerides. Eur. J. Pharm. Sci. 20, 91–97.

Khaled, K.A., El-Sayed, Y.M., Al-Hadiya, B.M., 2003. Disposition of the flavonoid quercetin in rats after single intravenous and oral doses. Drug Dev. Ind. Pharm. 29, 397–403.

Khoo, S.M., Shackleford, D.M., Porter, C.J., Edwards, G.A., Charman, W.N., 2003. Intestinal lymphatic transport of halofantrine occurs after oral administration of a unit-dose lipid-based formulation to fasted dogs. Pharm. Res. 20, 1460–1465.

Kim, J.K., Choi, S.J., Cho, H.Y., Hwang, H.J., Kim, Y.J., Lim, S.T., Kim, C.J., Kim, H.K., Peterson, S., Shin, D.H., 2010. Protective effects of kaempferol (3,4′,5,7-tetrahydroxyflavone) against amyloid beta peptide (Abeta)-induced neurotoxicity in ICR mice. Biosci. Biotechnol. Biochem. 74, 397–401.

Kwon, S.H., Nam, J.I., Kim, S.H., Kim, J.H., Yoon, J.H., Kim, K.S., 2009. Kaempferol and quercetin, essential ingredients in *Ginkgo biloba* extract, inhibit interleukin-1beta-induced MUC5AC gene expression in human airway epithelial cells. Phytother. Res. 23, 1708–1712.

Labbe, D., Provencal, M., Lamy, S., Boivin, D., Gingras, D., Beliveau, R., 2009. The flavonols quercetin, kaempferol, and myricetin inhibit hepatocyte growth factor-induced medulloblastoma cell migration. J. Nutr. 139, 646–652.

Lee, J.S., Lee, M.K., Ha, T.Y., Bok, S.H., Park, H.M., Jeong, K.S., Woo, M.N., Do, G.M., Yeo, J.Y., Choi, M.S., 2006. Supplementation of whole persimmon leaf improves lipid profiles and suppresses body weight gain in rats fed high-fat diet. Food Chem. Toxicol. 44, 1875–1883.

Liu, Y., Zhang, P., Feng, N., Zhang, X., Wu, S., Zhao, J., 2009. Optimization and in situ intestinal absorption of self-microemulsifying drug delivery system of oridonin. Int. J. Pharm. 365, 136–142.

Ma, C.Y., Musoke, S.F., Tan, G.T., Sydara, K., Bouamanivong, S., Southavong, B., Soejarto, D.D., Fong, H.H., Zhang, H.J., 2008. Study of antimalarial activity of chemical constituents from *Diospyros quaesita*. Chem. Biodivers. 5, 2442–2448.

Matsumoto, M., Kotani, M., Fujita, A., Higa, S., Kishimoto, T., Suemura, M., Tanaka, T., 2002. Oral administration of persimmon leaf extract ameliorates skin symptoms and transepidermal water loss in atopic dermatitis model mice, NC/Nga. Br. J. Dermatol. 146, 221–227.

Narang, A.S., Delmarre, D., Gao, D., 2007. Stable drug encapsulation in micelles and microemulsions. Int. J. Pharm. 345, 9–25.

Polli, J.E., Crison, J.R., Amidon, G.L., 1996. Novel approach to the analysis of *in vitro–in vivo* relationships. J. Pharm. Sci. 85 (7), 753–760.

Pouton, C., 1997. Formulation of self-emulsifying drug delivery systems. Adv. Drug Deliv. Rev. 25, 47–58.

Rogerio, A.P., Dora, C.L., Andrade, E.L., Chaves, J.S., Silva, L.F., Lemos-Senna, E., Calixto, J.B., 2010. Anti-inflammatory effect of quercetin-loaded microemulsion in the airways allergic inflammatory model in mice. Pharmacol. Res. 61, 288–297.

Schmidts, T., Nocker, P., Lavi, G., Kuhlmann, J., Czermak, P., Runkel, F., 2009. Development of an alternative, time and cost saving method of creating pseudoternary diagrams using the example of a microemulsion. Colloids Surf. A 340, 187–192.

Swenson, E., Curatolo, W., 1992. (C) Means to enhance penetration: (2) intestinal permeability enhancement for proteins, peptides and other polar drugs: mechanisms and potential toxicity. Adv. Drug Deliv. Rev. 8, 39–92.

Thuong, P.T., Lee, C.H., Dao, T.T., Nguyen, P.H., Kim, W.G., Lee, S.J., Oh, W.K., 2008. Triterpenoids from the leaves of *Diospyros kaki* (persimmon) and their inhibitory effects on protein tyrosine phosphatase 1B. J. Nat. Prod. 71, 1775–1778.

Wu, W., Wang, Y., Que, L., 2006. Enhanced bioavailability of silymarin by self-microemulsifying drug delivery system. Eur. J. Pharm. Biopharm. 63, 288–294.

Zhang, P., Liu, Y., Feng, N., Xu, J., 2008. Preparation and evaluation of self-microemulsifying drug delivery system of oridonin. Int. J. Pharm. 355, 269–276.

Zhao, D.L., Hirst, B.H., 1990. Comparison of bile salt perturbation of duodenal and jejunal isolated brush-border membranes. Digestion 47, 200–207.